Optics & Laser Technology 150 (2022) 107943

Contents lists available at ScienceDirect

Optics and Laser Technology

journal homepage: www.elsevier.com/locate/optlastec

15 Mbps underwater wireless optical communications based on acousto-optic modulator and NRZ-OOK modulation

Tao Wang [a], Bo Wang [a], Liqi Liu [a], Renjiang Zhu [a], Lijie Wang [b], Cunzhu Tong [b], Yanrong Song [c], Peng Zhang [d,*]

[a] College of Physics and Electronic Engineering, Chongqing Normal University, Chongqing 401331, People's Republic of China
[b] State Key Laboratory of Luminescence and Applications, Changchun Institute of Optics, Fine Mechanics and Physics, Chinese Academy of Sciences, Changchun, Jilin 130033, People's Republic of China
[c] College of Applied Sciences, Beijing University of Technology, Beijing 100124, People's Republic of China
[d] National Center for Applied Mathematics, Chongqing Normal University, Chongqing 401331, People's Republic of China

ARTICLE INFO

Keywords:
Underwater wireless optical communications
Acousto-optic modulator
NRZ-OOK
Modulation
Bit error rate

ABSTRACT

Communications with link distance of hundreds of meters and data rate of tens of Mbps are highly demanded in underwater wireless optical communications (UWOC) between autonomous underwater vehicles (AUVs) and submarines, or among others underwater platforms. In these cases, a high-power light source has to be used and an external modulation must be imposed. Here we present an UWOC system based on acousto-optic modulator (AOM), Non-Return-to-Zero On-Off Keying (NRZ-OOK) modulation and 520 nm green laser diode light source. A data rate of 15 Mbps, the highest reported values of an UWOC system using AOM to our best knowledge, with 9 m distance and 1.53×10^{-4} bit error rate (BER), as well as the longest distance of 18 m with 12 Mbps data rate and 4.7×10^{-3} BER are obtained in the tap water, in which an attenuation coefficient of 0.0503 m^{-1} for 520 nm wavelength is measured. By adding different dosages of Maalox suspension, different types of water quality are prepared, and the influences of Maalox concentration on the attenuation coefficient and the BER are investigated. It is found that increasing Maalox concentrations would worse the scatter effect of light beam, which further affect the transmission performance of the signal.

1. Introduction

The ocean covers about 71% of the earth's surface area, in which the rich biological and mineral resources have not been exploited yet. The key technology of marine exploration has subsequently become a frontier topic all over the world. Underwater wireless sensor networks, Internet of Underwater Things, as well as various autonomous underwater vehicles (AUVs) are widely used in underwater activities including data collection, environmental monitor and offshore oil exploration [1-3]. Therefore, a reliable underwater communication link plays a vital role in these underwater activities. At present, underwater communication systems are mainly divided into wired and wireless. The more mature wired communication technology uses cable or optical fiber for reliable communication, but its maintenance difficulties and limited mobility limit its underwater application. In contrast, as an efficient and convenient data transmission technology in modern ocean exploration, underwater wireless communication has gradually become the main development direction of underwater communication because of its more flexible and effective use. Conventional acoustic communication and radio frequency (RF) communication suffer limited bandwidth and high propagation latency which cannot meet certain applications that require large data volume and high data rate [4]. Thus, UWOC has attracted considerable attention in academic circles in recent years due to its rich spectrum resources, strong anti-interference ability and low cost [5-9].

Since blue-green (450–550 nm) visible light has lower attenuation optical window and stronger penetration in seawater, it is often used as a light source in UWOC system [10]. The realization of modulation in UWOC system mainly includes internal and external modulation. For internal modulation, the signal is directly input into the driving circuit of the light source, so to change the output characteristics of the beam. Many internal modulation related works have been reported, and they mainly focused on high-speed and low-power experiments. Hanson et al. developed a 1 Gbps UWOC system over a 2 m path in a laboratory water

* Corresponding author.
E-mail address: zhangpeng2010@cqnu.edu.cn (P. Zhang).

https://doi.org/10.1016/j.optlastec.2022.107943
Received 24 December 2021; Received in revised form 25 January 2022; Accepted 30 January 2022
Available online 5 February 2022

pipe [6]. Oubei et al. experimentally demonstrated a record 2.3 Gbps UWOC link over 7 m distance using a commercially available 12 mW green LD [11]. Xu et al. proposed a UWOC system based on a multi-pixel photon counter. By adopting 32-QAM OFDM signals, a 21 m, 312.03 Mbps underwater transmission is achieved [8]. Then, under the same low-power 520 nm LD, they used a frequency domain equalizer combined with a time-domain decision feedback noise predictor at the receiver to reduce inter-symbol interference for the first time, and finally successfully achieved a net rate of 3.31 Gbps and a transmission distance up to 56 m [9]. Although these internal modulation schemes have high data rate, they typically have low power and short transmission distances, making them more suitable for Underwater wireless sensor networks as well as Internet of Underwater Things. However, the research progress of LD driver based on high power and high data rate is slow, and it is a thorny problem to realize long-distance underwater communication through internal modulation of high current.

External modulation loads signals to the external modulation device, thereby changes the characteristics of beam passing through. Compare with electro-optic and magneto-optical external modulation, acousto-optic external modulation has a higher extinction ratio (generally greater than 1000:1), lower driving voltage, and higher temperature stability [12]. A free space optics (FSO) communication system using an acousto-optic modulator (AOM) has been proposed in literate [13]. Mesleh et al. theoretically studied an AOM-FSO system performance in the Gamma-Gamma turbulent channel, and their Monte Carlo simulation revealed that low bit error rate (BER) can be achieved at arbitrary low Signal-Noise Ratio values [14]. Xiao et al. designed a FSO system based on AOM, and 115.2 kbps communication has been achieved [15]. A. K. Ghosh et al. proposed an another AOM based FSO and data beam security was ensured through chaotic encryption technology [16]. This external modulation scheme is applicable to high-power light sources, thus extend the transmission distance and meet the communication between underwater mobile applications such as AUVs and submarines.

An AOM based UWOC has been mentioned by Longacre [17], but no experimental data about data rate or communication distance has been presented. So far, there are few studies on UWOC using external modulation and AOM. Compared with internal modulation, the advantage of external modulation is more suitable for high-power light source thus for hundreds of meters link distance and tens of Mbps data rate, which are highly demanded in UWOC between AUVs and submarines, or among others underwater platforms.

In this paper, we demonstrate a UWOC system based on external modulation and AOM that can potentially support tens of Mbps data rate and low BER performance, which is suitable for a relatively long communication distance. The measured attenuation coefficient (0.0503 m^{-1}) of tap water is equivalent to that of pure sea water, and the highest data rate of 15 Mbps and the longest distance of 18 m are performed. By adding different dosages of Maalox suspension into the tap water, four different water qualities (pure sea water, clear ocean water, coastal ocean water and turbid harbor water) are prepared respectively, and changes of beam scattering are studied under above four kinds of water qualities. The BER of the 12 Mbps UWOC link increases from 3.525×10^{-4} to 1.14×10^{-2} over 3 m Maalox underwater channel, and influences of water turbidity on communication performance are further confirmed. Our works provide a probably guideline for future real-time UWOC applications.

2. Experimental setup

2.1. Light source

The 520 nm laser diode used in this experiment is a common light source in UWOC at present. Fig. 1. (a) shows the output optical power versus driving current (P-I) at 20℃. The P-I curve is measured by an optical power meter (Thorlabs, PM100D). It can be seen that the threshold current of the LD is around 22 mA. When the current is 111 mA, the maximum power 15.26 mW can be obtained. Fig. 1. (b) shows the optical spectra under different drive currents measured using a HORIBA iHR320 spectrometer, and the full-width at half-maximum is approximately 0.24 nm. The peak emission wavelength is around 519.75 nm at 70 mA, and will slightly red-shifted with the increase of driving current.

2.2. Acousto-optic modulator

The basic structure of an AOM is composed of an acousto-optic crystal, a piezoelectric transducer and a driver. When the RF signal is loaded on the piezoelectric transducer, the piezoelectric transducer converts the electrical signal into an ultrasonic signal and transmits it to the acousto-optic crystal. The ultrasonic wave causes a periodic change of the refractive index of the acousto-optic crystal and forms a phase grating, usually called an ultrasonic grating. When the incident beam is at a certain angle of θ_B, Bragg diffraction will occur through the acoustic grating, and the phase and frequency of diffracted light will be changed [13,18], as shown in Fig. 2.

The Bragg diffraction angle θ_B can be written as [19]

$$\theta_B = arcsin\left(\frac{\lambda}{2n\lambda_s}\right) \tag{1}$$

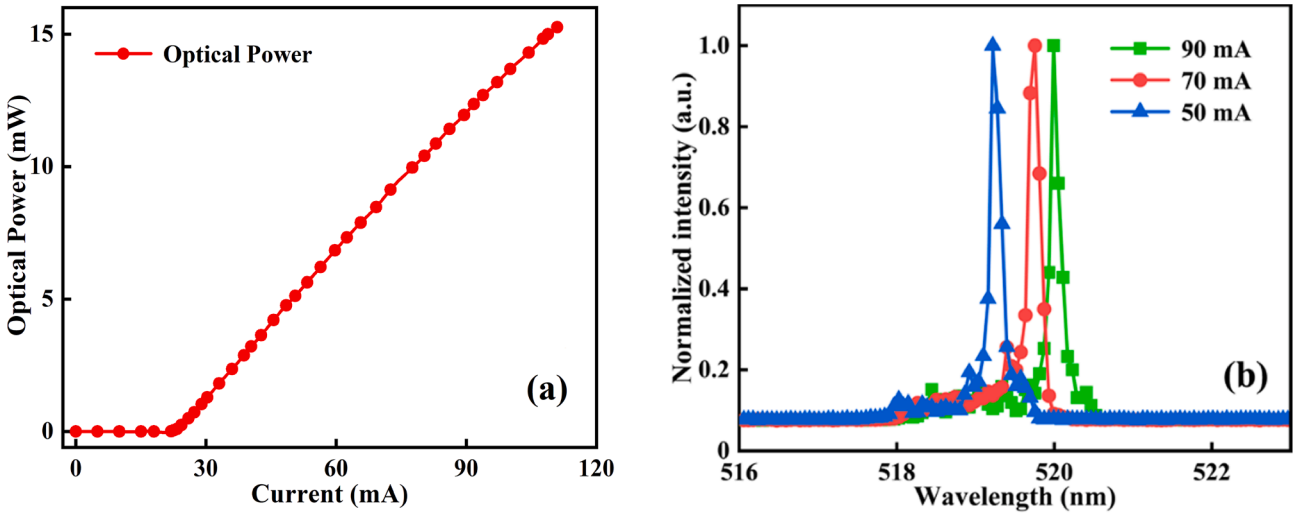

Fig. 1. P-I characteristics of the 520 nm LD at 20℃ (a), and the measured optical spectra for various bias currents (b).

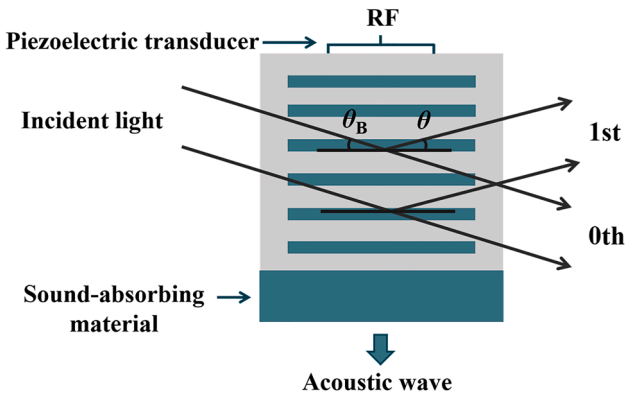

Fig. 2. Block diagram of acousto-optic Bragg modulation.

where λ is the incident light wavelength, n is the refractive index of acousto-optic crystal, and λ_S is the wavelength of ultrasonic. The diffraction efficiency of 1st diffracted light can be expressed as

$$\eta = sin^2\left(\frac{\pi}{\sqrt{2}\lambda}\sqrt{\frac{L}{H}M_2P_S}\right) \quad (2)$$

where P_s is the ultrasonic power, L and H are the length and width of the piezoelectric transducer, M_2 is the physical combination parameters of the acousto-optic crystal. The intensity of the diffracted light of Bragg diffraction is related to the intensity of the sound field and the characteristics of the acousto-optic crystal. Usually, by changing the P_s, the intensity of the diffracted light will change accordingly, which can achieve the purpose of improving the diffraction efficiency. The RF output of AOM driver is jointly controlled by two different modulation inputs, the analog and the digital modulation input. Among them, the analog modulation input can control the amplitude of RF signal output, thereby effectively adjusting the power of the ultrasonic wave to change the intensity of the diffracted light; while the digital modulation input a Transistor-Transistor Logic (TTL) signal, and its high and low levels are equivalent to a "switch" to control whether the RF signals output.

Fig. 3 illustrates the 250 MHz RF signals output after adding 0.8 V direct current power to the analog modulation input. The digital modulation input provides TTL rectangular waves (high level 4 V, low level 200 mV) of different frequencies, and it can be observed in Fig. 4 that the RF signal of the AOM driver changes with the TTL signals under different frequencies. When the frequency of the modulation signal is within 13 MHz, the high and low levels of RF signal are consistent with the duration of the high and low levels of the original TTL signal; beyond 13 MHz, the high and low levels of RF signal are inconsistent with the original TTL signal, which is determined by the performance of AOM driver.

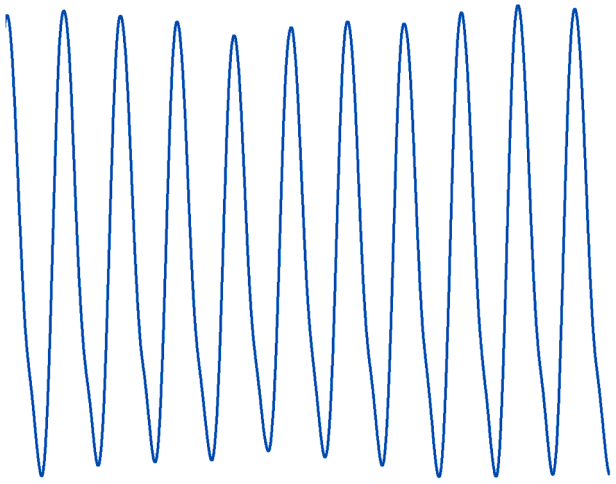

Fig. 3. 250 MHz RF signal output without TTL.

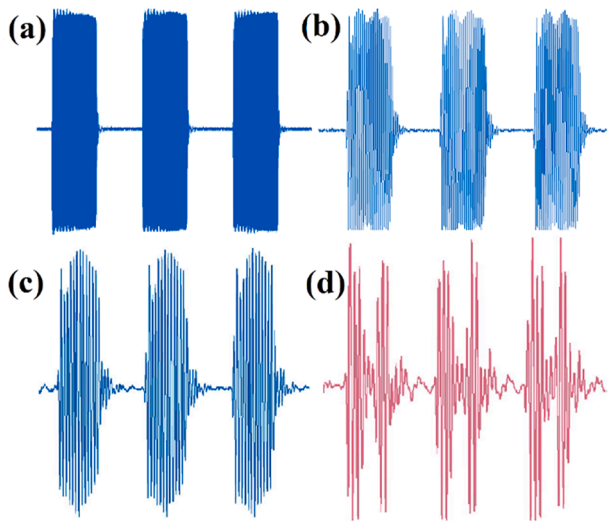

Fig. 4. 1 MHz (a), 5 MHz (b), 9 MHz (c) and 13 MHz (d) RF signals output with TTL signal.

2.3. Experimental setup

The schematics of the experimental UWOC system with a 520 nm laser diode based on AOM using NRZ-OOK modulation is shown in Fig. 5. A commercial single-mode fiber-pigtailed green-light LD (Thorlabs, LP520-SF15) is used as the transmitter and is mounted on a TEC module (Thorlabs, LDM9LP). The green laser beam is collimated by a fiber collimation package (Thorlabs, F260FC-A) to obtain a relatively longer transmission distance. Then, a pseudo-random binary sequence length of 2^{16} is generated offline by program and uploaded into a field-programmable gate array (FPGA, Cyclone IV EP4CE10F17C8). Next, the generated NRZ-OOK data signals with FPGA are loaded on AOM driver. In order to improve the diffraction efficiency of laser beam crossing the AOM, a small light spot should be forced to enter the AOM (SGT250-490–0.2TA), thus a convex lens with focal length of 18.4 mm is employed before the beam arriving AOM. At the same time, a 75 mm focal length lens is placed behind the AOM, which forms an inverted telescope system along with the above 18.4 mm lens, and allows the

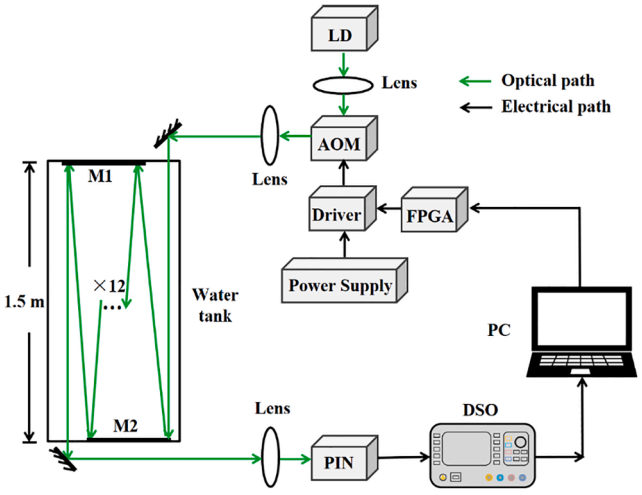

Fig. 5. Experimental setup for the UWOC system. M1: Mirror1, M2: Mirror2.

modulated laser beam travelling farther. A 1.5 m × 0.5 m × 0.5 m water tank is filled with tap water to build the underwater channel, and the underwater transmission distance can be adjusted by changing the numbers of reflection (up to 12 reflections) of light beam. At the receiver, the output beam is focused on a PIN photodetector (Thorlabs, PDA10A2) by a convex lens, and the detected electrical signals are captured by a Digital Oscilloscope (DSO), then sent to the PC for further processing.

The key sections of the AOM based UWOC experimental setup are shown in Fig. 6. Fig. 6(a) shows the optical parts of the transmitter including a green LD with a fiber collimation package, a front convex lens, an acousto-optic crystal and a rear convex lens. In order to reduce the attenuation of light during transmission, a large mirror (254 mm width, 100 mm height) with 97% reflectivity is attached to the outside of the water tank, and five small mirrors (30 mm width, 30 mm height) with same reflectivity are installed at the opposite end inside the water tank, so to adjust the light path and form different transmission distances. A total of 18 m distance can be achieved by fine-tuning the angle of the light beam as shown in Fig. 6(b). Fig. 6(c) indicates the PIN set at the other end outside of the tank, and Fig. 6(d) depicted the entire UWOC system.

3. Results and discussion

The performance of a UWOC system will be affected by the light sources, the used modulation techniques and the detectors. Meanwhile, the impact of the underwater channels also plays an important role. In this work, we experimentally study the performance of an AOM-based UWOC system in different underwater channels, and the influences of Maalox concentration on the attenuation coefficient and the BER are investigated.

3.1. Under tap water

We firstly intestate an AOM-based UWOC system in tap water. The output power $P_T(\lambda)$ of an incident light beam (at wavelength λ and with power $P_I(\lambda)$) after passing through the water body can be calculated as [4]

$$P_T(\lambda) = P_I(\lambda) - P_A(\lambda) - P_S(\lambda) \quad (3)$$

where $P_A(\lambda)$ is absorbed power and $P_S(\lambda)$ is scattered power. Beer-Lambert law describes the attenuation of light beams underwater as [20,21]

$$P_T(\lambda) = P_I(\lambda)\exp(-c(\lambda)l) \quad (4)$$

where $c(\lambda)$ stands for the extinction coefficient after propagating distance l.

The measured received optical power versus different transmission distance is shown in Fig. 7. According to the fitted curve, the attenuation coefficient $c(\lambda)$ is 0.0503 m^{-1}. The received optical power at 3 m and 18

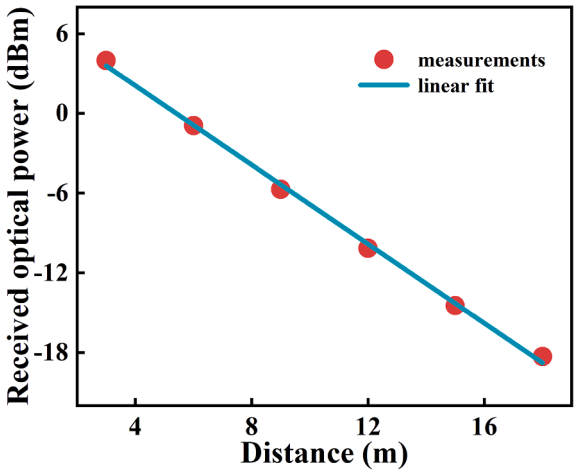

Fig. 7. The received optical power versus transmission distance under tap water.

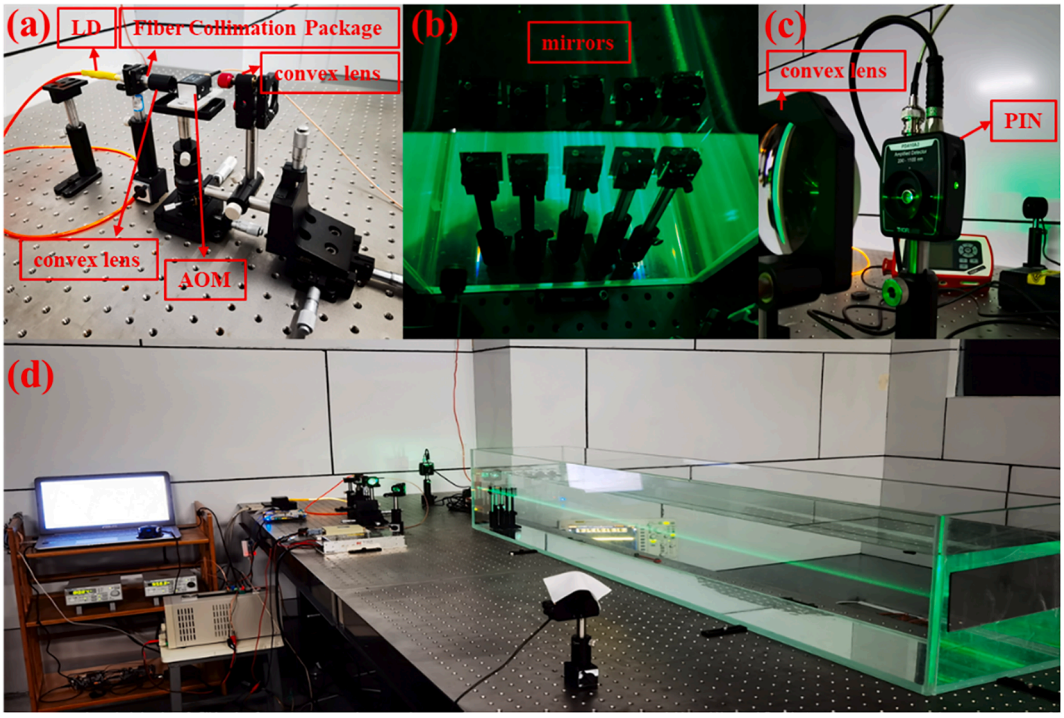

Fig. 6. Key sections of the UWOC system: transmitter (520 nm laser with a fiber collimation package, AOM and lens) (a), mirrors (b), PIN (c), and the whole UWOC system (d).

m distance are 3.98 dBm and −18.30 dBm, respectively. Fig. 8 shows the BERs curves of the 12 Mbps signal versus transmission distance. It can be seen that BER increases with longer transmission distance. The longest distance of 18 m with 12 Mbps data rate and 4.7×10^{-3} BER are obtained. The BER of 12 m tap water is 2.17×10^{-3}, and the corresponding eye diagram, which is captured by a mixed signal oscilloscope (Tektronix MSO68B with the sampling rate of 50 Gs/s), is shown as the inset.

Fig. 9 shows the BER curves versus optical power for various data rates after a 9 m tap water. It can be found that the changing trend of BER under three data rates is consistent: the BER will decrease when the received optical power keep increasing. As the transmission rate is 5 Mbps, we achieve a BER of 1.53×10^{-4} at received optical power of −5.37 dBm, and when the data rate increases to 15 Mbps, the minimum received optical power of −4.41 dBm should be used to achieve the same BER. The highest data rate of 15 Mbps in this work is mainly limited by the output power of the used green LD and the modulation bandwidth of the AOM driver.

For actual applications such as UWOC between AUVs and submarines, or among others underwater platforms, in which hundreds of meters transmission distance are needed, a higher output power light source must be employed. It can be estimated that for a 200 m communication distance, an 8.4 W power LD should be applied if the 15 Mbps date rate, the 1.53×10^{-4} BER and the minimum −4.41 dBm received optical power are still wanted.

NRZ-OOK signal is electrically amplified by 25 dB gain using an amplifier (Mini-Circuit ZHL-6A-S +) to increase the RF signal power and improve the extinction ratio. The measured eye diagrams by the use of a MSO68B at different data rates under 9 m water channel are shown in Fig. 10, and it can be concluded that the eye diagrams decrease with the increase of transmission rate.

3.2. Under water with Maalox solution

Tang et al. theoretically studied the inter-symbol interference caused by multipath scattering in turbid seawater such as coastal and harbor water, and found that multipath scattering will seriously degrades the BER performance for high data rate UWOC systems with OOK modulation [22]. Light scattering in water is caused by non-algae suspended particles, and the scattering process and mechanism are relatively complex. For the sake of simplicity, Maalox suspension composed mainly of $Mg(OH)_2$ and $Al(OH)_3$ is usually added to water to simulate non-algae suspended particles, so as to study the scattering effect of non-algae suspended particles in seawater [23-25]. The water turbidity is changed by adding the Maalox solution 10 ml steps. To quantify the turbidity of water, we use Beer-Lambert law to calculate the corresponding attenuation coefficient, and the results are shown in Fig. 11. The calculated attenuation coefficients of water vary range from 0.0503 m^{-1} to 2.186 m^{-1}, covering pure sea water, clear ocean water, coastal ocean water and turbid harbor water [6]. Fig. 12(i)-(l) show side views of green light passing through water bodies with different turbidities taken by a camera under same exposure setting. We can find that as the dosage of the Maalox solution (namely the turbidity) increases, the caused light scattering effect becomes stronger.

When the Maalox solutions are added to 0.089, 0.178, 0.267, 0.356, 0.446 and 0.535 mg/L, the received optical powers are 2.91, 2.79, 2.45, 1.98, 1.68 and 1.30 dBm, respectively. The corresponding BERs of the 12 Mbps NRZ-OOK signals, which are arisen from the scattering of Maalox are presented in Fig. 13. It can be seen in Fig. 13 that the BER of 12 Mbps signal over a 3 m underwater channel is 3.06×10^{-3} with 0.356 mg/L Maalox solution, and the measured attenuation coefficient is 0.367 m^{-1}. It is clear that the turbidity of the water has indeed a significant impact on the communication performance. For further reduced BERs, a higher power light source and a more sensitive detector should be chosen.

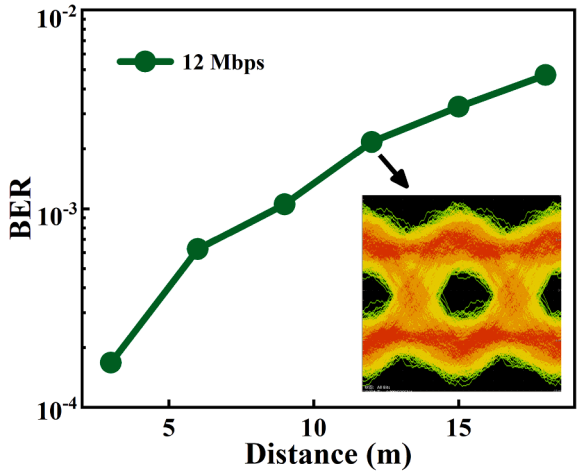

Fig. 8. BERs of the 12 Mbps signal versus transmission distance. The corresponding eye diagram is shown as the inset.

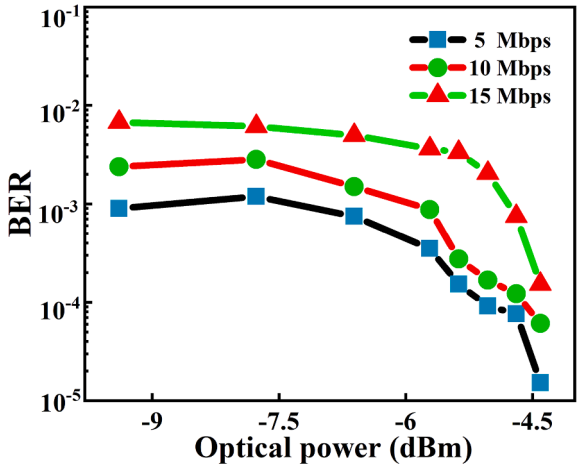

Fig. 9. BER curves versus optical power at 5, 10, 15 Mbps after a 9 m transmission.

4. Conclusions

We have demonstrated a stable UWOC system based on an AOM and a single-mode pigtailed 520 nm green LD using NRZ-OOK modulation. The data rate up to 15 Mbps with 9 m link distance and 1.53×10^{-4} BER, and the communication distance up to 18 m with 12 Mbps data rate and 4.7×10^{-3} BER are achieved in the tap water. The influences of Maalox concentration on the attenuation coefficient and the BER are also investigated using our self-made different types of water quality, and it is found that increasing Maalox concentrations will aggravate the scatter effect of light beam even further and degrade the transmission performance of the signal. Although the link distance in the experiment is not large enough due to the power limitation of the used green LD, however, our experiment verifies the feasibility of a UWOC based on AOM for the first time. The communication distance of such a system can be improved to hundreds of meters by adding the output power of the light source, which may find many application scenarios such as UWOC between AUVs and submarines, or among others underwater platforms.

CRediT authorship contribution statement

Tao Wang: Conceptualization, Methodology, Software, Investigation, Formal analysis, Writing – original draft. **Bo Wang:** Data curation, Writing – original draft. **Liqi Liu:** Visualization, Investigation. **Renjiang**

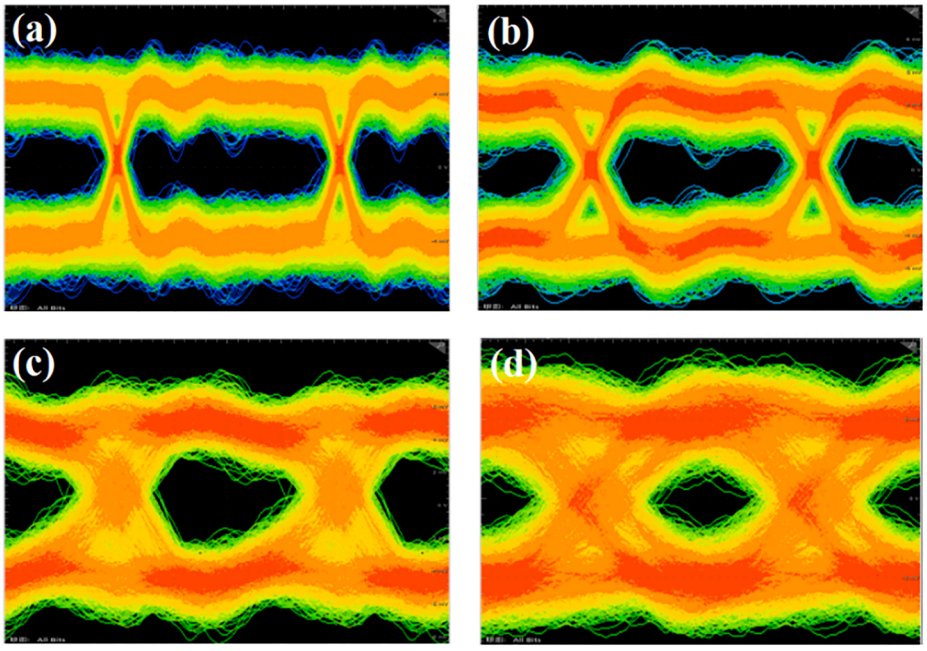

Fig. 10. Eye diagrams of the 5 Mbps (a), 10 Mbps (b), 15 Mbps (c) and 20 Mbps (d) NRZ-OOK signals after 9 m tap water channel.

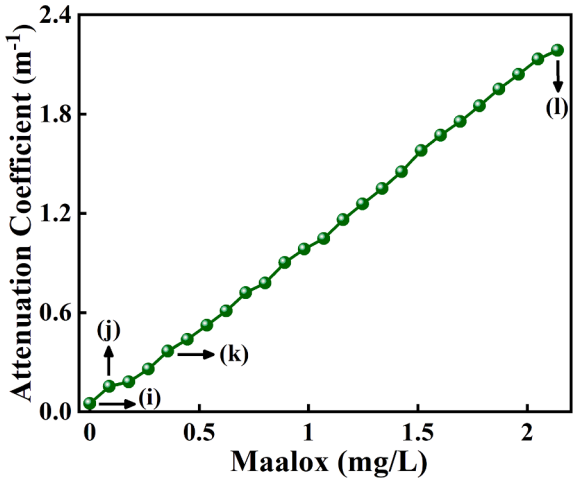

Fig. 11. Attenuation coefficient versus the added Maalox solution.

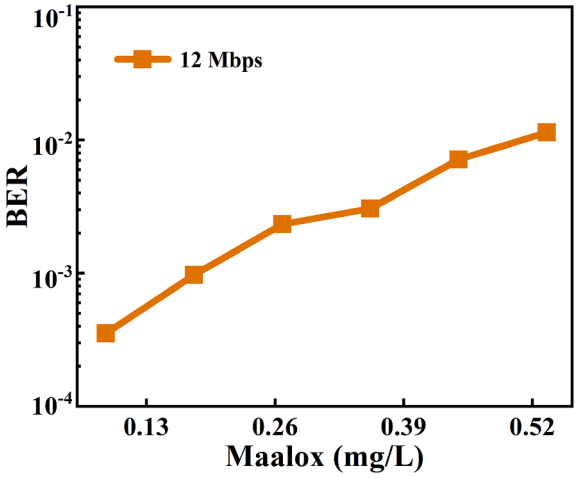

Fig. 13. BERs of the 12 Mbps signal versus Maalox concentration.

Zhu: Resources, Supervision. **Lijie Wang:** Software, Validation. **Cunzhu Tong:** Software, Validation. **Yanrong Song:** Formal analysis. **Peng Zhang:** Conceptualization, Funding acquisition, Resources, Supervision,

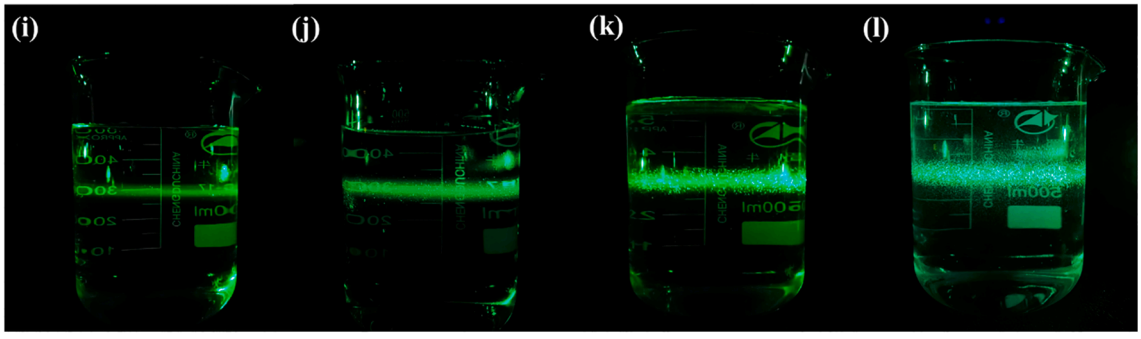

Fig. 12. The snapshots of the optical beam passing through water with different turbidities: pure sea water (i), clear ocean water (j), coastal ocean water (k) and turbid harbor water (l).

Writing – review & editing.

Declaration of Competing Interest

The authors declare that they have no known competing financial interests or personal relationships that could have appeared to influence the work reported in this paper.

Acknowledgements

This work is supported by the National Natural Science Foundation of China (61904024), the Cooperation project between Chongqing local universities and institutions of Chinese Academy of Sciences, the Chongqing Municipal Education Commission (HZ2021007), the Science and Technology Research Program of Chongqing Municipal Education Commission (KJZD-M201900502), and the State Key Laboratory of Luminescence and Applications (SKLA-2019-04).

References

[1] J.J. Li, D.M. Ye, K. Fu, L.N. Wang, J.L. Piao, Y.J. Wang, Single-photon detection for MIMO underwater wireless optical communication enabled by arrayed LEDs and SiPMs, Opt. Express 29 (16) (2021) 25922–25944, https://doi.org/10.1364/OE.433798.

[2] Z. Zeng, S. Fu, H. Zhang, Y. Dong, J. Cheng, A survey of underwater optical wireless communications, IEEE Commun. Surv. Tutorials 19 (1) (2017) 204–238, https://doi.org/10.1109/COMST.2016.2618841.

[3] M. Singh, M.L. Singh, G. Singh, H. Kaur, Priyanka, S. Kaur, Real-time image transmission through underwater wireless optical communication link for Internet of Underwater Things, Int. J. Commun. Syst. 34 (16) (2021), https://doi.org/10.1002/dac.v34.1610.1002/dac.4951.

[4] H. Kaushal, G. Kaddoum, Underwater optical wireless communication, IEEE Access 4 (2016) 1518–1547, https://doi.org/10.1109/ACCESS.2016.2552538.

[5] M. Kong, B. Sun, R. Sarwar, J. Shen, Y. Chen, F. Qu, J. Han, J. Chen, H. Qin, J. Xu, Xu, Underwater wireless optical communication using a lens-free solar panel receiver, Opt. Commun. 426 (2018) 94–98, https://doi.org/10.1016/j.optcom.2018.05.019.

[6] F. Hanson, S. Radic, High bandwidth underwater optical communication, Appl. Opt. 47 (2) (2008) 277–283, https://doi.org/10.1364/AO.47.000277.

[7] J.M. Wang, C.H. Lu, S.B. Li, Z.Y. Xu, 100 m/500 Mbps underwater optical wireless communication using an NRZ-OOK modulated 520 nm laser diode, Opt. Express 27 (9) (2019) 12171–12181, https://doi.org/10.1364/OE.27.012171.

[8] J.L. Wang, X.Q. Yang, W.C. Lv, C.Y. Yu, J.Y. Wu, M.M. Zhao, F.Z. Qu, Z.W. Xu, J. Han, J. Xu, Underwater wireless optical communication based on multi-pixel photon counter and OFDM modulation, Opt. Commun. 451 (2019) 181–185, https://doi.org/10.1016/j.optcom.2019.06.053.

[9] X. Chen, W. Lyu, Z. Zhang, J. Zhao, J. Xu, 56-m/331-Gbps underwater wireless optical communication employing Nyquist single carrier frequency domain equalization with noise prediction, Opt. Express 28 (16) (2020) 23784, https://doi.org/10.1364/OE.399794.

[10] S.Q. Duntley, Light in the Sea, J. Opt. Soc. Am. 53 (2) (1963) 214–233, https://doi.org/10.1364/JOSA.53.000214.

[11] H.M. Oubei, C. Li, K.-H. Park, T.K. Ng, M.-S. Alouini, B.S. Ooi, 23 Gbit/s underwater wireless optical communications using directly modulated 520 nm laser diode, Opt. Express 23 (16) (2015) 20743, https://doi.org/10.1364/OE.23.020743.

[12] S.H. Xu, S.L. Xiao, A novel technique for duplex communication system with a signal-light source, Semicond. Optoelectron. 36 (3) (2015) 447–450, https://doi.org/10.13756/j.gtxyj.2014.05.018.

[13] R. Mesleh, A. AL-Olaimat, Acousto-Optical Modulators for Free Space Optical Wireless Communication Systems, J. Opt. Commun. Netw. 10 (5) (2018) 515, https://doi.org/10.1364/JOCN.10.000515.

[14] R. Mesleh, A. AL-Olaimat, Performance Analysis of Acousto Optical Modulator–Free Space Optical System Over Gamma–Gamma Turbulent Channel, 2019 International Symposium on Networks, Computers and Communications (ISNCC). (2019) 1-6, https://doi.org/10.1109/ISNCC.2019.8909148.

[15] S.H. Xu, S.L. Xiao, S. Wang, X. Yi, Research on AOM-based modulation technology for laser communications, Study Opt. Commun. 5 (185) (2014) 59–62, https://doi.org/10.3756/j.gtxyj.2014.05.018.

[16] A.K. Ghosh, P. Verma, S. Cheng, R.C. Huck, M.R. Chatterjee, M. Al-Saedi, Design of Acousto-optic Chaos based Secure Free-space Optical Communication Links, Proc. SPIE Int. Soc. Opt. Eng. 7464 (2009) 74640L, https://doi.org/10.1117/12.826813.

[17] J. R. Longacre, D. Freeman, J. B. Snow, High data rate underwater laser communications, Proc. SPIE Int. Soc. Opt. Eng. 1302 (1990) 433–439, https://doi.org/10.1117/12.21462.

[18] M. Eghbal, J. Abouei, Security Enhancement in Free-Space Optics Using Acousto-Optic Deflectors, J. Opt. Commun. Network. 6 (8) (2014) 685–694, https://doi.org/10.1364/JOCN.6.000684.

[19] V. Nikulina, R. Khandekara, J. Sofka, G. Tartakovsky, Acousto-optic pointing and tracking systems for free-space laser communications, Proc. SPIE Int. Soc. Opt. Eng. 5892 (2005) 58921C, https://doi.org/10.1117/12.617498.

[20] T. Hamza, M.A. Khalighi, S. Bourennane, P. Leon, J. Opderbecke, Investigation of solar noise impact on the performance of underwater wireless optical communication links, Opt. Express 24 (22) (2016) 25832–25845, https://doi.org/10.1364/OE.24.025832.

[21] C.D. Mobley, B. Gentili, H.R. Gordon, Z. Jin, G.W. Kattawar, A. Morel, P. Reinersman, K. Stamnes, R.H. Stavn, Comparison of numerical models for computing underwater light fields, Appl. Opt. 32 (36) (1993) 7484, https://doi.org/10.1364/AO.32.007484.

[22] S.J. Tang, Y.H. Dong, X.D. Zhang, Impulse Response Modeling for Underwater Wireless Optical Communication Links, IEEE Trans. Commun. 62 (1) (2014) 226–234, https://doi.org/10.1109/TCOMM.2013.120713.130199.

[23] P.F. Tian, H.L. Chen, P.Y. Wang, X.Y. Liu, X.W. Chen, G.F. Zhou, S.L. Zhang, J. Lu, P.J. Qiu, Z.Y. Qian, X.L. Zhou, Z.L. Fang, L.R. Zheng, R. Liu, X.G. Cui, Absorption and scattering effects of Maalox, chlorophyll, and sea salt on a micro-LED-based underwater wireless optical communication [Invited], Chinese Opt. Lett. 17 (10) (2019), 100010, https://doi.org/10.3788/COL201917.100010.

[24] L. Mullen, B. Cochenour, W. Rabinovich, R. Mahon, J. Muth, Backscatter suppression for underwater modulating retroreflector links using polarization discrimination, Appl. Opt. 48 (2) (2010) 328–337, https://doi.org/10.1364/ao.48.000328.

[25] W. Cox, J. Muth, Simulating channel losses in an underwater optical communication system, J. Opt. Soc. Am. A. 31 (5) (2014) 920–934, https://doi.org/10.1364/JOSAA.31.000920.